

Comparison of Type 1 and 2 Choroidal Neovascularization Characteristics Using Optical Coherence Tomography Angiography in Age-Related Macular Degeneration

Ozlem BICER¹, Sibel DEMIREL², Figen SERMET³, Emin OZMERT³

ABSTRACT

Purpose: To compare the morphologic characteristics of type 1 and 2 choroidal neovascularization (CNV) in exudative age-related macular degeneration (AMD) patients with optical coherence tomography angiography (OCTA).

Materials and Methods: OCTA imaging of 36 eyes of 36 patients (24 type 1 CNV, 12 type 2 CNV) with AMD under follow-up in our clinic were reviewed retrospectively. Neovascular complex were qualitatively and quantitatively analyzed at baseline and at follow-up visits.

Results: Mean follow-up time was 19.81±6.21 (12-31) months, and median number of injections was 6 (1-11). No significant difference was found for feeder vessel, branching numerous tiny capillaries, loops, peripheral arcade, loop and anastomoses between the groups. However, perilesional hypointense halo was seen more frequently in type 2 CNV group at baseline and final follow-up ($p=0,002$, $p=0,021$, respectively). GLD of CNV, selected CNV area and flow area measurements were found to be higher in type 1 CNV at baseline and follow-up ($p=0.004$, $p=0.001$, $p=0.002$, respectively) ($p<0,001$, $p<0,001$, $p<0,001$, respectively). There was no statistically significant changes in GLD of CNV, CNV area and flow area both type 1 CNV and type 2 CNV after treatment.

Conclusion: OCTA provides noninvasive imaging in differential diagnosis and follow-up of CNV subtypes secondary to AMD. Type 2 CNV was characterized by smaller CNV area, flow area and GLD of CNV compared with type 1 CNV. The GLD of CNV, selected CNV area and flow area in both groups showed no significant change from baseline after PRN treatment at least more than 1 year of follow-up.

Keywords: Age-related macular degeneration, Choroidal neovascularization, Type 1 choroidal neovascularization, Type 2 neovascularization, Optical coherence tomography angiography

INTRODUCTION

In developed countries, age-related macular degeneration (AMD) is one of the leading causes of severe loss of vision over 60 years of age. Although wet type AMD characterized by choroidal neovascularization (CNV) accounts for 10-15% of all cases, it accounts for 88% of severe loss of vision.¹ Gass classified CNV lesions into two groups based on anatomic and angiographic appearance. The neovascularization located under the retinal pigment epithelium (RPE) which characterized by less leakage is termed as type 1 CNV while it passes through the RPE, compromising the neurosensory retina which characterized by intense leakage is termed as type 2 CNV.² Fluorescein angiography (FA) has been used as gold standard in the

diagnosis and follow-up; the introduction of OCT has facilitated diagnosis and monitoring activity.³ Due to the limitations in dye-based angiography, our knowledge about the responses and anatomical changes of CNV subtypes in AMD to antivascular endothelial growth factor (anti-VGEF) treatment is limited. Optical coherence tomography angiography (OCTA) is a novel imaging modality that provides structural information about retinal and choroidal vessels without need for intravenous contrast agent. Owing to no staining and no leakage on OCTA, vascular structures are not masked by hyperfluorescence, and vascular network can be visualized with more details.^{4,5}

For OCTA, sensitivity ranges from 50% to 86.5% while specificity ranges from 67.6% to 100% for detection

1- Ophthalmologist, MD. Ankara University Faculty of Medicine, Department of Ophthalmology, Ankara, Turkey

2- Associate Prof., MD. Ankara University Faculty of Medicine, Department of Ophthalmology, Ankara, Turkey

3- Prof., MD. Ankara University Faculty of Medicine, Department of Ophthalmology, Ankara, Turkey

Received: 28.11.2019

Accepted: 31.08.2020

Ret-Vit 2021; 30: 13-21

DOI:10.37845/ret.vit.2021.30.3

Correspondence Address:

Ozlem BICER

Ankara University Faculty of Medicine,
Department of Ophthalmology, Ankara, Turkey

Phone:

E-mail: ozlembicer90@gmail.com

of CNV.^{6,7} However, the combination of FA with OCT (sensitivity: 92.72% and specificity: 90.91%) increased sensitivity and specificity when compared to use of OCTA alone (sensitivity: 85.62% and specificity: 81.51%).⁸ Also, combination of OCTA with structural OCT increased sensitivity from 66.7% to 85.7% when compared to use of OCTA or FA alone.⁹ Currently, OCTA analysis is increasingly used to assess morphological characteristics before and after anti-VGEF therapy in CNV subtypes seen in AMD.¹⁰⁻¹⁵ The lesions can be assessed as immature, mature or hyper-mature based on its maturity; however, they can also termed as dense, loose, mixed vascular network and unidentifiable CNV pattern based on morphology of vascular network as well.^{10,11} Recent studies have described OCTA images of CNV lesion as having glomeruli, sea-fan, medusa, lacywheel, indistinct, pruned vascular tree, tangled vascular network, vascular loop and so on.¹²⁻¹⁶ Among these, glomeruli pattern was solely described in type 2 CNV lesions.¹⁴ Although there are studies suggesting that there is no difference between CNV subgroups regarding vascular pattern, data is still insufficient in this issue.¹⁷ However, there is limited number of studies about the changes in CNV morphology and changes in CNV size in response to anti-VEGF treatment between the groups. In this study, it was aimed to compare long-term OCTA findings in cases on intravitreal anti-VGEF therapy with type 1 and type 2 CNV secondary to wet type AMD.

MATERIALS AND METHODS

We retrospectively reviewed clinical records of 36 eyes (24 eyes with type 1 CNV and 12 eyes with type 2 CNV) 36 patients with diagnosis of wet type AMD who were followed in our clinic between March, 2016 and May, 2019. The study was approved by Ethics Committee of Ankara University. The study was conducted in accordance to tenets of Helsinki Declaration. In all patients included, lesions were classified as type 1 and type 2 CNV based on FA images at time of presentation.

The study included patients with clinically active or inactive wet type AMD who were on Pro re nata (PRN) anti-VGEF regimen with at least 12 months and had initial OCTA imaging study providing detailed images of neovascular network. The exclusion criteria were presence of CNV secondary to another retinal disease, presence of other macular abnormalities (diabetic retinopathy, arterial or venous occlusions, high myopia) that may affect interpretation of images, absence of CNV on initial OCTA, and poor image quality with a signal strength index <45. In addition, inactive lesions with scarring and those not received treatment for at least.

6 months were also excluded. Previous anti-VGEF therapy was not considered as exclusion criteria.

In all patients, records of detailed ophthalmological examination, best-corrected visual acuity (BCVA) and ETDRS (Early Treatment Diabetic Retinopathy Study) score were available. Again, baseline SD-OCT (Spectralis, Heidelberg, Germany), OCTA (Angiovue RTVue XR Avanti; Optovue, California, USA) and FA (Heidelberg Retina Angiograph 2, Heidelberg, Germany) were also available for all patients. Baseline and final OCT and OCTA images were assessed. The last control visit with available OCTA image was considered end of follow-up.

The OCTA images were acquired by RTVue XR Avanti device using split-spectrum-amplitude-decorrelation algorithm. This system utilizes an A-scan rate of 70.000 scans per second, a light source centered on 840 nm and a bandwidth 50 nm. Each OCTA volume contained 304x304 A scans and used 2 consecutive B scans. Each OCTA volume, is acquired in 3 seconds, and 2 orthogonal OCTA volumes were acquired to perform motion correction to minimize motion artifacts arising from microsaccades and fixation changes. All OCTA images (6x6 mm scan area) were interpreted by a retina specialist (S.D) experienced in ocular imaging. Based on literature, qualitative parameters were defined as presence of visible feeder vessel, branching numerous tiny capillaries, peripheral arcade, loop, anastomosis and hypo-intense halo.^{12,13} Miere et al. classified neovascular membrane into 4 morphological patterns as seafan, medusa, indistinct and pruned vascular tree.¹² Based on the study, central feeder, circular peripheral anastomosis, thin branches and surrounding hypo-intense halo were observed in medusa pattern while eccentric feeder vessel, thin branches and surrounding hypo-intense halo was observed in sea-fan pattern. In indistinct pattern, no feeder vessel was observed but surrounding hypo-intense halo and circumferential peripheral anastomosis can be seen in addition to thin branches. In pruned vascular tree pattern, feeder vessel can be seen; however, thin branches are lacking and there is filamentous flow. The cases displaying suspected activation areas during follow-up were assigned into pruned vascular tree pattern because predominant filamentous flow. In our study, morphological classification was made by taking these patterns into consideration. Thereafter, the lesion was considered active on OCTA if at least 3 of 5 criteria were present, which were described to determine OCTA activation of CNV by Coscas et al.¹³ Accordingly, CNV lesion was defined as active if at least 3 of 5 criteria including sea-fan or lacywheel pattern, peripheral anastomosis/loop, peripheral arcade, hypo-intense halo and branching numerous tiny capillaries (Chart 1). In our study, active lesion patterns defined by Coscas et al. were modified as sea-fan, medusa and indistinct patterns.

Chart 1. Active and inactive lesion criteria described by Coscas et al.

	Active	Inactive
Shape	Lacy-wheel or sea-fan	Long, filamentous vessels
Branching pattern	Multiple, branching, tiny capillaries	Large, mature vessels
Presence of anastomosis and loop	Abundant	Rare
Vessel termination	Peripheral arcuate	Dead tree appearance
Hypo-intense halo	Present	Absent

Quantitatively, CNV area on outer retina or choriocapillaris layer was manually measured and selected CNV area, flow area and greatest linear diameter (GLD) of lesion were recorded. On OCT, central macular thickness (CMT) was calculated by the device as the average value in the central 1-mm diameter area of the ETDRS macular map automatically provided. After treatment, the relationship between change in CNV size on OCTA and change in CMT on OCT were analyzed.

Statistical analyses were performed using SPSS version 20.0 (SPSS, Inc.). Data are summarized using descriptive statistics including mean, standard deviation, minimum, maximum and percent. Categorical variables are presented as frequency and percent while continuous variables are presented as mean \pm standard deviation. Qualitative data were compared using Pearson Chi-square or Fisher's exact test between groups. Pre-treatment and post-treatment qualitative data were compared using Exact McNemar test.

Quantitative data were compared between groups using Mann Whitney U test while intra-group comparisons were performed using Wilcoxon significance test. Spearman's correlation analysis was used to determine whether there was a correlation between change in CMT on OCT and changes in selected CNV area or flow area. Concordance between OCT and OCT was assessed using Cohen's kappa coefficient. A p value < 0.05 was considered as statistically significant.

RESULTS

The study included 36 eyes of 36 patients (28 men, 8 women, mean age: 71.42 \pm 8.55 years). It was found that there was type 1 CNV in 24 eyes (66.7%) and type 2 CNV in 12 eyes (33.3%). During follow-up, PRN anti-VEGF regimen was given to all patients. At baseline, 4 cases in type 1 CNV group and 1 case in type 2 CNV were inactive according to OCT. Table 1 presents demographic and clinical characteristics of the patients. Mean follow-up was 19.81 \pm 6.21 months (12-31 months).

At baseline, it was found that there was sea-fan pattern in 3 (12.5%), medusa pattern in 11 (45.8%) and pruned vascular tree pattern in 3 (12.5%) of cases with type 1 CNV while there was sea-fan pattern in 3 (25.0%), medusa pattern in 1 (8.3%) and pruned vascular tree pattern in 8 (66.7%) of cases with type 2 CNV (Figure 1 and 2). At last follow-up, it was seen that there was a change to pruned vascular tree pattern from medusa pattern in 2 cases with type 1 CNV and to medusa pattern from indistinct pattern in 1 case with type 1 CNV. In addition, 1 case with type 2 CNV, no flow signal was detected on OCTA at the last follow-up (Figure 3). When morphological patterns on baseline OCTA were compared between groups, it was found that indistinct pattern was significantly more frequent in cases with type 2 CNV (p=0.036). No significant difference was detected

Table 1. Demographic and clinical characteristics of cases.

	Type 1 CNV	Type 2 CNV	Total
Gender (F/M)	8/16	0/12	8/28
Mean age (year), (range)	71.29 \pm 9.52 (52-89)	71.67 \pm 6.54 (57-80)	71.42 \pm 8.55 (52-89)
Side (right/left)	13/11	8/4	21/15
Number of anti-VEGF injections before baseline, median, (range)	11 (3-38)	7.5 (3-25)	10 (3-38)
Mean follow-up (mo), (range)	20.92 \pm 6.07 (12-31)	17.58 \pm 6.14 (12-31)	19.81 \pm 6.21 (12-31)
Number of anti-VEGF injections during follow-up, median, (range)	6 (1-11)	4.5 (1-8)	6 (1-11)
Mean BCVA at baseline, logMAR	0.63 \pm 0.48 (0.1-2.1)	0.59 \pm 0.33 (0.1-1.0)	0.61 \pm 0.43 (0.1-2.1)
Mean final BCVA, logMAR	0.69 \pm 0.55 (0.1-2.1)	0.68 \pm 0.31 (0.2-1.0)	0.68 \pm 0.48 (0.1-2.1)

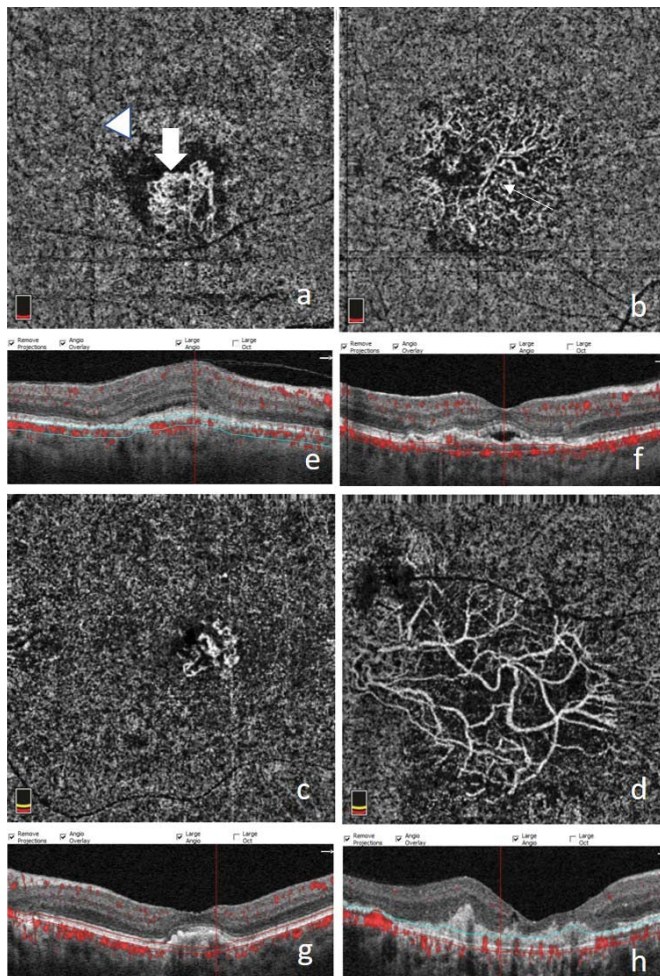


Figure 1: a, b, c, d: Optical coherence tomography angiography (OCTA) images; e, f, g, h: B-scan OCT images. a) sea-fan pattern b) medusa pattern c) indistinct pattern, d) pruned vascular tree pattern. e: type 2 CNV f, g, h: type 1 CNV. Thin arrow: feeder vessel, thick arrow: peripheral arcade, arrow head: hypo-intense halo surrounding lesion.

CNV: choroidal neovascularization

between groups regarding morphological CNV patterns on final OCTA ($p=0.100$). At last follow-up, it was seen that, of the cases with pruned vascular tree pattern, 1 (20%) was inactive while 4 (80%) were active (Figure 4 and 5).

No significant difference was found between groups regarding presence of visible feeder vessel, branching tiny capillaries, peripheral anastomosis, peripheral arcade and loop at baseline or last follow-up ($p>0.05$). Both at baseline and final visit, hypo-intense halo was found to be significantly more common in cases with type 2 CNV ($p=0.002$ and $p=0.021$, respectively). Table 2 and 3 summarize qualitative parameters on OCTA.

In both type 1 and type 2 CNV groups, no significant difference was found regarding presence of visible feeder

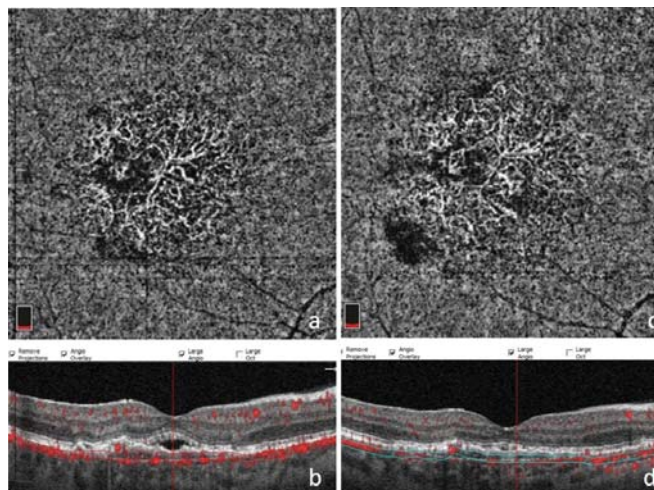


Figure 2: 61-years old male, right eye a, c: Optical coherence tomography angiography (OCTA) images; b, d: B-scan OCT images. a) Medusa pattern is seen in type 1 CNV case underwent 13 anti-VEGF injections on baseline OCTA imaging. b) Subretinal fluid is seen B-scan OCT c) Medusa pattern is seen in the patient underwent 7 anti-VEGF injections after mean follow-up of 16 months d) Complete regression of fluid is seen in B-scan OCT.

CNV: choroidal neovascularization

Anti-VEGF: Anti-vascular endothelial growth factor

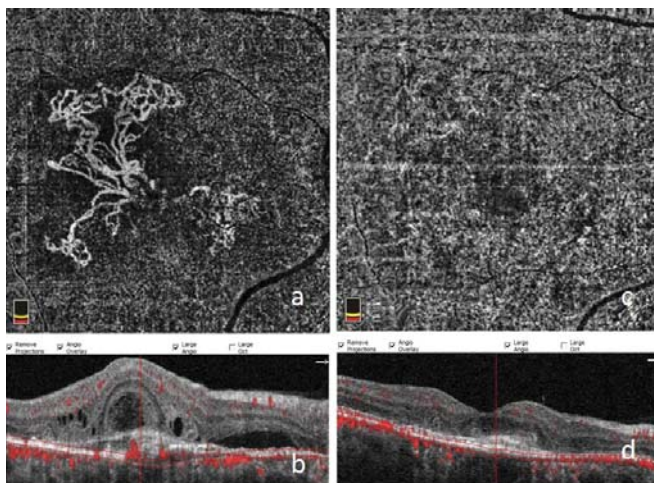


Figure 3: 71-years old male, right eye a, c: Optical coherence tomography angiography (OCTA) images; b, d: B-scan OCT images. a) Medusa pattern is seen in type 2 CNV case underwent 3 anti-VEGF injections on baseline OCTA imaging. b) Subretinal and intraretinal fluid is seen B-scan OCT c) It is seen that CNV was disappeared in the patient underwent 6 anti-VEGF injections after mean follow-up of 11 months. d) Complete regression of fluid is seen in B-scan OCT

CNV: choroidal neovascularization

Anti-VEGF: Anti-vascular endothelial growth factor

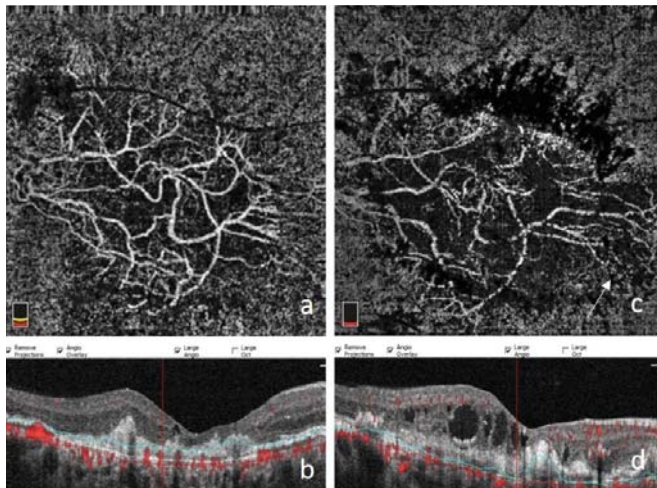


Figure 4: 54-years old male, right eye **a, c:** Optical coherence tomography angiography (OCTA) images, **b, d:** B-scan OCT images. **a)** Pruned vascular tree pattern is seen type 1 CNV case underwent 3 anti-VEGF injections on baseline OCTA imaging. **b)** Minimal intraretinal cysts are seen in B scan OCT **c)** Despite minimal increase in capillarity (arrow), pruned vascular tree pattern is seen in the patient underwent 6 anti-VEGF injections after mean follow-up of 20 months

d) Increased intraretinal cysts are seen in B scan OCT. CNV: choroidal neovascularization

Anti-VEGF: Anti-vascular endothelial growth factor

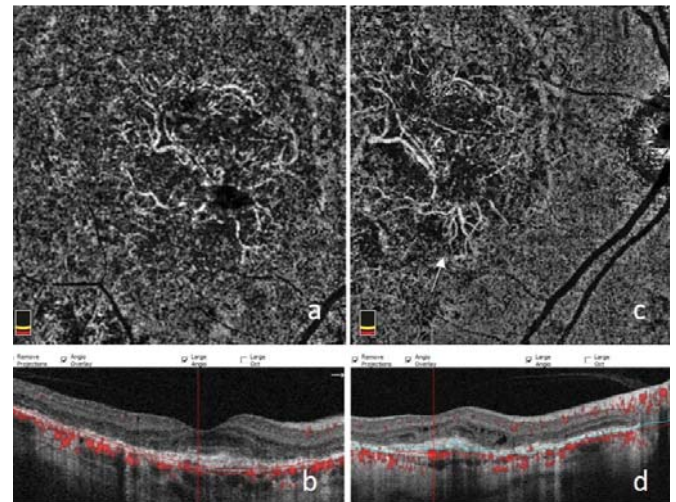


Figure 5: 64-years old male, right eye **a, c:** Optical coherence tomography angiography (OCTA) images, **b, d:** B-scan OCT images. **a)** Pruned vascular tree pattern is seen type 1 CNV case underwent 8 anti-VEGF injections on baseline OCTA imaging **b)** Minimal intraretinal cysts are seen in B scan OCT **c)** Despite minimal increase in capillarity (arrow), pruned vascular tree pattern is seen in the patient underwent 4 anti-VEGF injections after mean follow-up of 12 months

d) Increased intraretinal cysts are seen in B scan OCT. CNV: choroidal neovascularization

Anti-VEGF: Anti-vascular endothelial growth factor

Table 2. Qualitative parameters on baseline OCTA.

	Type 1 CNV	Type 2 CNV	P value
Feeder vessel, n (%)	10 (41.7%)	3 (25%)	0.468
Branching, numerous tiny capillaries. n (%)	21 (87.5%)	9 (75%)	0.378
Peripheral anastomosis. n (%)	18 (75%)	9 (75%)	1.000
Peripheral arcade. n (%)	5 (20.8%)	2 (16.7%)	1.000
Loop. n (%)	1 (4.2%)	3 (25%)	0.098
Hypo-intense halo. n (%)	2 (8.3%)	7 (58.3%)	0.002
Morphological pattern. n (%)			
o Sea-fan	3 (12.5%)	3 (25%)	0.036
o Medusa	11 (45.8%)	1 (8.3%)	
o Indistinct	7 (29.2%)	8 (66.7%)	
o Pruned vascular tree	3 (12.5%)	0 (0%)	

Table 3. Qualitative parameters on final OCTA.

	Type 1 CNV	Type 2 CNV	P value
Feeder vessel, n (%)	11 (45.8%)	3 (27.3%)	0.461
Branching, numerous tiny capillaries. n (%)	19 (79.2%)	9 (81.8%)	1.000
Peripheral anastomosis. n (%)	17 (70.8%)	5 (45.5%)	0.258
Peripheral arcade. n (%)	6 (25%)	1 (9.1%)	0.392
Loop. n (%)	3 (12.5%)	1 (9.1%)	1.000
Hypo-intense halo. n (%)	2 (8.3%)	5 (45.5%)	0.021
Morphological pattern. n (%)			
o Sea-fan	3 (12.5%)	2 (18.2%)	0.100
o Medusa	10 (41.7%)	2 (18.2%)	
o Indistinct	6 (25%)	7 (63.6%)	
o Pruned vascular tree	5 (20.8%)	0 (0%)	

vessel, branching tiny capillaries, peripheral anastomosis, peripheral arcade and loop at last follow-up ($p > 0.05$).

Table 4 presents quantitative OCTA parameters in the patients. At baseline, it was found that GLD of CNV, selected CNV area and flow area were significantly greater in type 1 CNV compared to type 2 CNV ($p = 0.004$, $p = 0.001$ and $p = 0.002$, respectively). At last follow-up, it was found that GLD of CNV, selected CNV area and flow area were significantly greater in type 1 CNV compared to type 2 CNV ($p < 0.001$, $p < 0.001$ and $p < 0.001$, respectively) (Table 4). No significant difference was detected regarding GLD of CNV, selected CNV area and flow area between baseline and last follow-up in both type 1 CNV and type 2 CNV groups ($p > 0.05$).

At baseline, 12 (75%) of active type 1 CNV cases according to OCT were also active on OCTA while 5 (25%) were inactive. At last follow-up, 12 (75%) of active type 1 CNV cases according to OCT were also active on OCTA while 4 (25%) were inactive. At baseline, 9 (81.8%) of active type 2 CNV cases according to OCT were also active on OCTA while 2 (18.2%) were inactive. At last follow-up,

6 (85.7%) of active type 2 CNV cases according to OCT were also active on OCTA while 1 (14.3%) was inactive (Table 5 and Table 6). The concordance between OCT and OCTA was not significant neither type 1 CNV group nor type 2 CNV group at baseline ($p = 1.00$; $p = 0.07$). At last follow-up, no concordance was observed between OCT and OCTA in type 1 CNV group ($p = 0.01$) while there was moderate concordance in type 2 CNV group ($p = 0.023$; $Kappa = 0.657$).

No significant correlation was detected between quantitative CMT change and changes in selected CNV area and flow area in both type 1 and type 2 CNV groups ($p > 0.05$).

DISCUSSION

In the literature, it has been shown that OCTA can provide detailed description of CNV-related vascularity in AMD without need for intravenous contrast agent.^{4,9} There are contradictory results regarding changes in morphological characteristics of CNV after treatment.^{6,10,18} In this study, morphological changes and quantitative analyses were

Table 4. Quantitative parameters of baseline and final OCTA.

		Type 1 CNV	Type 2 CNV	P value
GLD of CNV. mm	Baseline	1.54±0.54	0.95±0.48	0.004
		1.59 (0.62-2.49)	0.90 (0.38-2.08)	
	Final	1.67±0.57	0.86±0.36	<0.001
		1.66 (0.57-2.87)	0.94 (0.00-1.33)	
Selected CNV area. mm ²	Baseline	5.83±4.06	1.90±1.72	0.001
		5.53 (0.65-15.97)	1.32 (0.27-6.01)	
	Final	6.74±4.50	1.71±1.00	<0.001
		5.20 (0.80-16.18)	1.67 (0.00-3.46)	
Flow area. mm ²	Baseline	3.33±2.22	1.17±0.96	0.002
		3.08 (0.42-9.07)	0.95 (0.19-3.26)	
	Final	3.89±2.49	1.07±0.67	<0.001
		3.00 (0.48-9.52)	1.04 (0.00-2.29)	

Table 5. Activity of type 1 and Type 2 CNV cases on baseline OCT and OCTA.

	OCTA		
	Type 1 CNV		
		Active	Inactive
OCT	Active	15 (75%)	5 (25%)
	Inactive	3 (75%)	1 (25%)
	Type 2 CNV		
		Active	Inactive
	Active	9 (81.8%)	2 (18.2%)
	Inactive	0 (0%)	1 (100%)

Table 6. Activity of type 1 and Type 2 CNV cases on final OCT and OCTA.

	OCTA		
	Type 1 CNV		
		Active	Inactive
OCT	Active	12 (75%)	4 (25%)
	Inactive	6 (75%)	2 (25%)
	Type 2 CNV		
		Active	Inactive
	Active	6 (85.7%)	1 (14.3%)
	Inactive	1 (25%)	3 (75%)

assessed in choroidal vascular membranes by OCTA in both type 1 CNV and type 2 CNV cases on active PRN regimen. It was reported that type 1 CNV lesion was greater than type 2 CNV lesions with less demarcated border and type 1 CNV lesion could be seen more clearly at choriocapillaris layer.¹⁹ In another study reported by Zhao et al., it was found that GLD, flow area and greatest vascular caliber were smaller in type 2 CNV compared to type 1 CNV. Authors also found that there was no significant difference in sea-fan, medusa and indistinct patterns between type 1 and type 2 CNV.¹⁷ This finding was confirmed with the study of Malamos et al. and they reported that sea-fan pattern was most common by 50% incidence among all patients.²⁰

In our study, we found that type 2 CNV lesions were smaller than type 1 lesions in compatible with the current literature. The most common pattern was medusa in type 1 CNV cases (45.8%) whereas indistinct pattern in type 2 CNV cases (66.7%). The reason why this pattern is more common in type 2 CNV cases might be explained previous anti-VEGF therapy and different morphological classification. However only difference we noticed except for the size of membranes is dark halo around type 2 CNV. Jia et al. reported that exudative changes lead blood flow alterations in choriocapillaris and darkening on OCTA images as a result of mechanic compression in choriocapillaris.²¹ However, it was reported that dark halo was observed in cases without subretinal/intraretinal fluid.²² Thus, it is not appropriate to associate presence of halo solely with activity. Halo appearance can result from lower flow rate at lesion margin and projection artifacts.²² Marques et al. suggested hypointense halo appearance around lesion on OCTA as fibrovascular capsule.²³ Approximately 25 years ago, Gass reported green-gray, black halo or plaque surrounding type 2 neovascular membrane on fundus examination, which result from proliferation of RPE.²⁴ In our study, type 2 CNV cases contain more hypo-intense halo than type 1 CNV cases. This difference might be related to the proliferation of RPE cells around neovascular complex extending subretinal area.

Miere and colleagues investigated qualitative and quantitative CNV changes after anti-VEGF therapy in treatment-naïve (undergoing the monthly anti-VEGF loading phase) and treated eyes (undergoing an as needed PRN regimen) with AMD using OCTA. The authors found no significant difference in both treatment-naïve and previously treated AMD patients regarding high flow vascular network, branching, feeder vessel, anastomotic arcade, dark halo, flow void and arteriolized vessel. Although no significant change was observed in CNV

area in PRN group, a significant decrease was seen in CNV area in patients received anti-VEGF loading dose.²⁵ In our study, similar to these results it was found that no qualitative or quantitative changes occurred at long-term in CNV cases receiving PRN regimen. This may be explained by maturation and abnormalization of neovascular vessels treated with continuous anti-VEGF therapy. This results were the same for both type 1 CNV and type 2 CNV cases.

In our study, it was found that there was no significant relationship between CMT and selected CNV area and flow area in both groups. Additionally, our results suggest that there may not always concordance between OCT and OCTA for daily clinical practice, combination of en face OCTA and structural OCT will be clinically more helpful in follow-up of CNV. With OCTA multiple different metrics are available for CNV for quantification. More advanced technologies are required to evaluate the morphologic and quantitative biomarkers of activity to better guide the treatment and to more accurately assess the angiographic response.

In studies assessing treatment response by OCTA, it was reported that reduction in CNV size was observed at short-term after treatment while there was no significant change and even an increase in CNV area at long-term.^{5,10,18} Short term response after loading dose in treatment naïve group was well demonstrated in McClintic's study. They found that CNV vessel and membrane areas were significantly reduced at follow-up visit month 3; however, both membrane area and vessel area showed no significant changes after 12 months of treatment.²⁶ In a retrospective study, which involved 42 treatment-naïve exudative AMD patients, Kim et al. analyzed lesion size and vascular density at baseline and after 12 months of treatment by OCTA. They showed that the mean lesion size in type 2 CNV group significantly decreased from $1.23 \pm 0.99 \text{ mm}^2$ at baseline to $0.79 \pm 0.61 \text{ mm}^2$ at 12 months. On the contrary, the mean lesion size in type 1 CNV group showed no significant change from baseline ($2.12 \pm 1.01 \text{ mm}^2$) after treatment at months 12 ($2.08 \pm 0.91 \text{ mm}^2$). No significant difference was reported in vessel density in both type 1 CNV and type 2 CNV groups.²⁷ Even if both type-1 and type-2 cases were treatment naïve cases in this study, the reason for different treatment response and decreasing size of the membranes for type 2 CNV might be secondary to the location of type 2 CNV which is above RPE layer. This difference may be associated with anti-VEGF concentration and vessel maturation. The concentration of anti-VEGF agents could be different for subretinal and sub-RPE neovascularization. However this result should be supported by further studies evaluating type 2 CNV with OCTA.

In accordance with previous long term results of anti-VEGF treatment we found that selected CNV area and flow area showed no significant changes for both groups after treatment. This result may be associated with the pruning process by anti-VEGF treatment for CNV. Although anti-VEGF agents inhibit both angiogenesis and vascular permeability, arteriogenesis mechanisms is one of the reason underlying lack of change in area and flow in long-term. Angiogenesis is regulated by balance between proangiogenic and anti-angiogenic factors. In this process, neovascular homeostasis is achieved by production of antiangiogenic factors and pruning of vessels. Spaide defined 'vascular normalization' as large diameter and prominent anastomoses in AMD patients who received repeated anti-VEGF injections and attributed vascular normalization to the important mechanism of arteriogenesis which is defined as the expansion of previously formed vessels.²⁸ During the natural course of neovascular AMD, neovascular remodeling by up-regulation platelet-derived growth factor-B pericyte coverage, which results increased vessel diameter. This can explain why lesion area and flow area do not change despite inactivation of lesion after treatment. Several studies in the literature seem supportive for this assumption.^{23,29}

Karaçorlu and colleagues described OCTA features of type 1 and type 2 CNV in AMD. In that study, the patients were divided into 3 groups: treatment-naïve with an active neovascular membrane, eyes receiving ongoing anti-VEGF treatments for active neovascular membrane and eyes with an inactive neovascular membrane treated with anti-VEGF at least 6 months ago. The lesions seafan and medusa patterns were classified as well-defined while those with death tree and pruned vascular tree patterns were classified as ill-defined patterns. They noted that long filamentous pattern was solely seen inactive neovascular membrane and it was assumed that this finding associated with chronicity and lesion inactivity.³⁰ In contrast to their result, we found that pruned vascular tree pattern was seen in both active and inactive CNV lesions. Thus, it seems that it is not reasonable to make a treatment decision solely based on CNV pattern. Filamentous pattern may not be detected due to the limited number of cases undergoing PRN. The limitations of this study include small sample size and lack of treatment-naïve eyes. Nevertheless, our results were similar with literature. In conclusion, our results suggest that previously treated cases may show different treatment response at long-term follow-up when compared to treatment-naïve patients.

REFERENCES

1. Ferris FL, 3rd, Fine SL, Hyman L. Age-related macular degeneration and blindness due to neovascular maculopathy. *Arch Ophthalmol.* 1984;102:1640-2.
2. Grossniklaus HE, Gass JD. Clinicopathologic correlations of surgically excised type 1 and type 2 submacular choroidal neovascular membranes. *Am J Ophthalmol.* 1998;126:59-69.
3. Chen CY, Wong TY, Heriot WJ. Intravitreal bevacizumab (Avastin) for neovascular age-related macular degeneration: a short-term study. *Am J Ophthalmol.* 2007;143:510-2.
4. Iafe NA, Phasukkijwatana N, Sarraf D. Optical Coherence Tomography Angiography of Type 1 Neovascularization in Age-Related Macular Degeneration. *Dev Ophthalmol.* 2016;56:45-51.
5. Kuehlewein L, Bansal M, Lenis TL, et al. Optical Coherence Tomography Angiography of Type 1 Neovascularization in Age-Related Macular Degeneration. *Am J Ophthalmol.* 2015;160:739-48.
6. Perrott-Reynolds R, Cann R, Cronbach N, et al. The diagnostic accuracy of OCT angiography in naïve and treated neovascular age-related macular degeneration: a review. *Eye (Lond).* 2019;33:274-82.
7. Turgut B. Optical Coherence Tomography Angiography – A General View. *European Ophthalmic Review.* 2016;10:39-42.
8. Souedan V, Souied EH, Caillaux V, et al. Sensitivity and specificity of optical coherence tomography angiography (OCT-A) for detection of choroidal neovascularization in real-life practice and varying retinal expertise level. *Int Ophthalmol.* 2018;38 38:1051-60.
9. Carnevali A, Cicinelli MV, Capuano V, et al. Optical Coherence Tomography Angiography: A Useful Tool for Diagnosis of Treatment-Naïve Quiescent Choroidal Neovascularization. *Am J Ophthalmol.* 2016;169:189-98.
10. Xu D, Davila JP, Rahimi M, et al. Long-term Progression of Type 1 Neovascularization in Age-related Macular Degeneration Using Optical Coherence Tomography Angiography. *Am J Ophthalmol.* 2018;187:10-20.
11. Sulzbacher F, Pollreisz A, Kaider A, et al; Vienna Eye Study Center. Identification and clinical role of choroidal neovascularization characteristics based on optical coherence tomography angiography. *Acta Ophthalmol.* 2017;95:414-20.
12. Miere A, Butori P, Cohen SY, et al. Vascular Remodeling of Choroidal Neovascularization after Anti-Vascular Endothelial Growth Factor Therapy Visualized on Optical Coherence Tomography Angiography. *Retina.* 2019;39:548-57.
13. Coscas GJ, Lupidi M, Coscas F, et al. Optical Coherence Tomography Angiography Versus Traditional Multimodal Imaging in Assessing the Activity of Exudative Age-Related Macular Degeneration: A New Diagnostic Challenge. *Retina.* 2015;35:2219-28.
14. El Ameen A, Cohen SY, Semoun O, et al. Type 2 neovascularization secondary to age-related macular degeneration imaged by optical coherence tomography angiography. *Retina.* 2015;35:2212-8.

15. Miere A, Semoun O, Cohen SY, et al. Optical Coherence Tomography Angiography Features of Subretinal Fibrosis in Age-Related Macular Degeneration. *Retina*. 2015;35:2275–84.
16. Turgut B. Retinal Hastalıklarda Optik Koherens Tomografi Anjiyografi. *Güncel Retina*. 2017;1:69-74.
17. Zhao Z, Yang F, Gong Y, et al. The Comparison of Morphologic Characteristics of Type 1 and Type 2 Choroidal Neovascularization in Eyes with Neovascular Age-Related Macular Degeneration using Optical Coherence Tomography Angiography. *Ophthalmologica*. 2019;13:1-9.
18. Pilotto E, Frizziero L, Daniele AR, et al. Early OCT angiography changes of type 1 CNV in exudative AMD treated with anti-VEGF. *Br J Ophthalmol*. 2019;103:67-71.
19. Farecki ML, Gutfleisch M, Faatz H, et al. Characteristics of type 1 and 2 CNV in exudative AMD in OCT-Angiography. *Graefes Arch Clin Exp Ophthalmol*. 2017;255:913-21.
20. Malamos P, Tsolkas G, Kanakis M, et al. OCT-Angiography for monitoring and managing neovascular age-related macular degeneration. *Curr Eye Res*. 2017;42:1689-97.
21. Jia Y, Bailey ST, Wilson DJ, et al. Quantitative optical coherence tomography angiography of choroidal neovascularization in age-related macular degeneration. *Ophthalmology*. 2014;121:1435–44.
22. Inoue M, Jung JJ, Balaratnasingam C, et al; COFT-1 Study Group. A Comparison Between Optical Coherence Tomography Angiography and Fluorescein Angiography for the Imaging of Type 1 Neovascularization. *Invest Ophthalmol Vis Sci*. 2016;57:314-23.
23. Marques JP, Costa JF, Marques M, et al. Sequential Morphological Changes in the CNV Net after Intravitreal Anti-VEGF Evaluated with OCT Angiography. *Ophthalmic Res*. 2016;55:145-51.
24. Gass JD. Biomicroscopic and histopathologic considerations regarding the feasibility of surgical excision of subfoveal neovascular membranes. *Trans Am Ophthalmol Soc*. 1994;92:91-111.
25. Miere A, Oubraham H, Amoroso F, et al. Optical Coherence Tomography Angiography to Distinguish Changes of Choroidal Neovascularization after Anti-VEGF Therapy: Monthly Loading Dose versus Pro Re Nata Regimen. *J Ophthalmol*. 2018;2018:3751702.
26. McClintic SM, Gao S, Wang J, et al. Quantitative Evaluation of Choroidal Neovascularization under Pro Re Nata Anti-Vascular Endothelial Growth Factor Therapy with OCT Angiography. *Ophthalmol Retina*. 2018;2:931-41.
27. Kim JM, Cho HJ, Kim Y, et al. Responses of Types 1 and 2 Neovascularization in Age-Related Macular Degeneration to Anti-Vascular Endothelial Growth Factor Treatment: Optical Coherence Tomography Angiography Analysis. *Semin Ophthalmol*. 2019;34:168-76.
28. Spaide RF. Optical Coherence Tomography Angiography Signs of Vascular Abnormalization With Antiangiogenic Therapy for Choroidal Neovascularization. *Am J Ophthalmol*. 2015;160:6-16.
29. Lumbroso B, Rispoli M, Savastano MC. Longitudinal Optical Coherence Tomography-Angiography Study of Type 2 Naive Choroidal Neovascularization Early Response After Treatment. *Retina*. 2015;35:2242-51.
30. Karacorlu M, Sayman Muslubas I, Arf S, et al. Membrane patterns in eyes with choroidal neovascularization on optical coherence tomography angiography. *Eye (Lond)*. 2019;33:1280-9.